

Supporting Information

Interfacial Assembly of Lipopeptide Surfactants on Octyltrimethoxysilane Modified Silica Surface

Jiqian Wang^{1*}, Donghui Jia^{1,2}, Kai Tao¹, Chengdong Wang¹, Xiubo Zhao³,
Mohammed Yaseen², Hai Xu¹, Guohe Que¹, John R. P. Webster⁴, and Jian R Lu^{2*}

¹State Key Laboratory of Heavy Oil Processing and Centre for Bioengineering and Biotechnology,
China University of Petroleum (East China), 66 Changjiang West Road, Qingdao 266555, China

²Biological Physics, School of Physics and Astronomy, University of Manchester, Schuster
Building, Manchester M13 9PL, UK

³Department of Chemical and Biological Engineering, University of Sheffield, Mappin Street,
Sheffield, S1 3JD, UK

⁴ISIS Neutron Facility, Rutherford Appleton Laboratory, Science and Technology Facilities
Council, Chilton, Didcot, Oxfordshire OX11 0QZ, UK

* Correspondence should be made to: Jiqian Wang, Tel: (+86)532-8698-1569, E-mail:
jqwang@upc.edu.cn, and Jian R. Lu, Tel: (+44)-161-306-3926, E-mail: j.lu@manchester.ac.uk

Theory of neutron reflection

Neutron reflection (NR) has been extensively used for determining the thickness and composition of interfacial layers adsorbed from surfactants, peptides, polymers and proteins.¹ Like X-ray reflection, neutrons have short wavelengths of a few angstroms, making it inherently sensitive to the determination of molecular structures. Unlike X-rays, however, the neutron signal arising from reflection is sensitive to deuterium labeling. The reflection of neutrons at surface or interface can be similarly described by the same equations as used for light. In specular reflection, these equations depend only on the refractive index profile normal to the surface, which in turn depends on the coherent scattering length density. The scattering length density profile derives from the chemical composition and density of scattering species. Hence detailed information about the interfacial region may be determined.

In a neutron reflection experiment, the reflectivity, R , is measured as a function of the wave vector transfer, κ , perpendicular to the reflecting surface, where

$$\kappa = \frac{4\pi \sin \theta}{\lambda} \quad (\text{s1}),$$

where θ is the incidence angle and λ the wavelength of the incidence neutron beam. R is equal to the ratio of the intensities between reflected ($I_{\text{ref}(\kappa)}$) and incident ($I_{\text{inc}(\kappa)}$) beams and in kinematic approximation² it is given as

$$R = I_{\text{ref}(\kappa)} / I_{\text{inc}(\kappa)} \approx \frac{16\pi^2}{\kappa^2} |\rho(\kappa)|^2 \quad (\text{s2}),$$

where $\rho(\kappa)$ is the one dimensional Fourier transform of the scattering length density profile (SLD), $\rho(z)$, normal to the interface:

$$\rho(\kappa) = \int_{-\infty}^{\infty} \exp(-i\kappa z) \rho(z) dz \quad (\text{s3}).$$

Thus, these equations show that through Fourier transform neutron reflectivity is related to the scattering length density across the interface. SLD or $\rho(z)$ is related to interfacial chemical composition through the following equation:

$$\rho(z) = \sum_{i=1}^m b_i n_i(z) \quad (\text{s4}),$$

where b_i is the scattering length and n_i is the number density of the i^{th} element in a given volume containing m different types of elements. Equation (s2) is only approximate because when κ becomes very low, it gives inadequate account of multiple scattering and the relationship tends to deviate or break down.

There is thus a direct relationship between the reflectivity profile and the scattering length density profile, and hence the composition profile normal to the interface. Although direct Fourier transform as described above can be pursued, the common difficulty lies in the phase resolution associated with the modulus squared term and because of the relatively narrow κ range over which the measurements are made.

It is often more convenient to use the optical matrix method³ to calculate the reflectivity exactly for any given model of the interface. Using this method, the calculated profile is compared with the measured profile and the process is repeated until an acceptable fit is obtained. The model typically consists of a series of layers, each with a scattering length density ρ_i and thickness τ_i , both of which are varied until the optimal fit to the data is found. Although any one profile is not necessarily a unique solution, different isotopic contrasts usually supply sufficient additional information to ensure the uniqueness of the interpretation.

Because different nuclei scatter neutrons with different amplitudes and in the case of proton and deuteron, with opposite phases, the use of a combination of protonated and deuterated materials can substantially change the reflectivity profile of a system while maintaining the same chemical structure. It is also possible, by adjustment of the H/D

ratio, to prepare solvents which are matched to the surface so that the contrast between surface and solvent is zero, giving a reflectivity profile arising only from the interfacial material.

Once the thickness and scattering length density for a given interfacial layer are defined, we can derive the volume fraction of the surfactant, ϕ_p , in the adsorbed layer

$$\phi_p = \frac{\rho - \rho_w}{\rho_{po} - \rho_w} \quad (s5),$$

where ρ_w is the scattering length density of D₂O ($=6.35 \times 10^{-6} \text{ \AA}^{-2}$), ρ_{po} is the scattering length density of fragment species in the layer and ρ is the fitted scattering length density. For a multilayer fit the weighted average scattering length density for the layers will give an overall volume fraction for the entire adsorbed layer. The area per molecule, A (in \AA^2), of surfactant can then be calculated from

$$A = \frac{V_{po}}{\tau \phi_p} \quad (s6),$$

where V_{po} is the volume of each layer fragment species (in \AA^3) and τ is the layer thickness (in \AA). Surface excess or adsorbed amount of each layer fragment species (in $\text{mg} \cdot \text{m}^{-2}$) can be obtained from

$$\Gamma = \frac{MW}{6.02A} \quad (s7),$$

where MW is the molecular weight of each layer fragment species (in $\text{g} \cdot \text{mol}^{-1}$).

For a multiple layer model fitting, the total surface excess or adsorbed amount should be the sum of surface excess or adsorbed amount of each layer fragment species. Subsequently, the area per molecule of the whole surfactant adsorbed at the solid/water interface can be calculated by equation (s7), but MW should be the molecular weight of species.

$$A_s = \frac{MW_s}{6.02\Gamma_{total}} \quad (s8)$$

In the case of a uniform model analysis without sensitivity to the separation between the tail and head group regions of the surfactant layer, water is freely associated with these regions and fills all gaps available. Thus, the structural parameters to be obtained must fulfill the following relations:

$$n_w = \frac{A_s \tau_{total} - V_s}{30}$$
$$\rho_i = \frac{b_i + n_w b_w}{A_s \tau_i} \quad (s9),$$
$$\phi_p = \frac{V_s}{A_s \tau_i}$$

In the case of adsorption of C₁₄K_n lipopeptide onto the hydrophobic C8/water interface, the most appropriate model that was found to fit the measured reflectivity profiles well consisted of a hydrophobic region close to the C8 surface and a hydrophilic peptide region into the bulk solution. All above equations apply to each region or layer given due consideration of segregation of acyl chain and peptide fragments and the number of water molecules associated with space filling.

References

1. Zhao, X.; Pan, F.; Lu, J. R., Interfacial assembly of proteins and peptides: recent examples studied by neutron reflection. *Journal of The Royal Society Interface* **2009**, *6* (Suppl 5), S659-S670.
2. Lu, J. R.; Lee, E. M.; Thomas, R. K., The Analysis and Interpretation of Neutron and X-ray Specular Reflection. *Acta Crystallographica Section A* **1996**, *52* (1), 11-41.
3. Heavens, O. S., Optical properties of thin films. *Reports on Progress in Physics* **1960**, *23*, 2-65.

Table S1. Physical parameters for C₁₄K_n lipopeptide surfactants

Sample fragments	Length 1 / Å	Volume V/ Å ³	Scattering length, b/10 ⁻⁵ /Å ⁻¹			Scattering length density, ρ/10 ⁻⁶ /Å ⁻²		
			D ₂ O	CMSi	H ₂ O	D ₂ O	CMSi	H ₂ O
hC ₁₄	19.21	404	-2.08	-2.08	-2.08	-0.05	-0.05	-0.05
dC ₁₄	19.21	404	278.99	278.99	278.99	6.90	6.90	6.90
K ₁	3	175.3	59.32	33.30	17.68	3.38	1.90	1.00
K ₂	6	350.6	116.70	64.70	33.48	3.33	1.85	0.95
K ₃	9	525.9	174.12	96.10	65.08	3.33	1.83	0.94
K ₄	12	701.6	231.52	127.5	65.08	3.30	1.82	0.93

Table S2 C₁₄K₁₋₄ structural parameters obtained from 1-layer model fitting to neutron reflectivity profiles measured at the C8/water interface. The C8 layer was determined from pure D₂O with τ=11±3 Å and ρ=1.4×10⁻⁶/Å⁻². All the measurements were made above CMC, at pH 6 and 22–23°C.

Sample	τ±2/ Å	(ρ _{po} ±0.1) ×10 ⁶ /Å ⁻²	(ρ _p ±0.1) ×10 ⁶ /Å ⁻²	ϕ _p ±0.05	Γ±0.15 /mg m ⁻²	A±2/ Å ²	n _w
hC ₁₄ hK ₁ (1CMC)	22	0.99	1.4	0.92	2.07	28.5	1.59
hC ₁₄ hK ₂ (1CMC)	21	1.5	1.6	0.98	2.19	36.6	0.46
hC ₁₄ hK ₃ (1.5CMC)	19	1.9	2.4	0.89	1.84	55.0	6.30
hC ₁₄ hK ₄ (1.5CMC)	19	2.1	3.0	0.79	1.70	73.7	9.84

Table S3 C₁₄K₁₋₄ structural parameters obtained from 2-layer model fitting to neutron reflectivity profiles measured at the C8/water interface. The C8 layer was determined from pure D₂O with τ=11±3 Å and ρ=1.4×10⁻⁶/Å⁻². All the measurements were made above CMC, pH 6 and at 22–23°C.

Sample	Layer	τ±2/ Å	(ρ _{po} ±0.1) ×10 ⁶ /Å ⁻²	(ρ _p ±0.1) ×10 ⁶ /Å ⁻²	ϕ _p ±0.05	Γ±0.15 /mg m ⁻²	Γ _{total} ±0.15 /mg m ⁻²	A±2/ Å ²
hC ₁₄ hK ₁ (1CMC)	hC ₁₄	17	-0.05	0.9	0.85	1.26	2.06	28.6
	hK ₁	10	3.38	4.6	0.59	0.80		
hC ₁₄ hK ₂ (1CMC)	hC ₁₄	13	-0.05	0.5	0.91	1.03	2.23	36.1
	hK ₂	13	3.33	4.2	0.71	1.20		
hC ₁₄ hK ₃ (1.5CMC)	hC ₁₄	10	-0.05	1.7	0.73	0.63	1.71	59.5
	hK ₃	12	3.33	4.2	0.71	1.08		
hC ₁₄ hK ₄ (1.5CMC)	hC ₁₄	9	-0.05	1.8	0.71	0.55	1.91	64.5
	hK ₄	14	3.30	4.0	0.77	1.36		

Table S4 $C_{14}K_1$ structural parameters obtained from 2-layer model fitting to neutron reflectivity profiles measured at the C8/water interface. The C8 layer was determined from pure D_2O with $\tau=11\pm3 \text{ \AA}$ and $\rho=1.4\times10^{-6}/\text{\AA}^2$. All the measurements were made at 1mM, pH 6 and at 22–23 °C.

Sample/contrast	Layer	$\tau\pm2/\text{\AA}$	$(\rho_{po}\pm0.1)\times10^{-6}/\text{\AA}^2$	$(\rho_p\pm0.1)\times10^{-6}/\text{\AA}^2$	$\phi_p\pm0.05$	$\Gamma\pm0.15/\text{mg m}^{-2}$	$\Gamma_{total}\pm0.15/\text{mg m}^{-2}$	$A\pm2/\text{\AA}^2$
h $C_{14}hK_1/D_2O$	h C_{14}	17	-0.05	0.9	0.85	1.26	2.06	28.6
	h K_1	10	3.38	4.6	0.59	0.80		
d $C_{14}hK_1/D_2O$	d C_{14}	17	6.91	6.8	0.82	1.36	2.08	30.5
	h K_1	8	3.38	4.4	0.66	0.72		
d $C_{14}hK_1/CMSi$	d C_{14}	17	6.91	6.0	0.81	1.35	2.06	30.8
	h K_1	8	1.90	1.96	0.65	0.71		

Table S5 $C_{14}K_2$ structural parameters obtained from 2-layer model fitting to neutron reflectivity profiles measured at the C8/water interface. The C8 layer was determined from pure D_2O with $\tau=11\pm3 \text{ \AA}$ and $\rho=1.4\times10^{-6}/\text{\AA}^2$. All the measurements were made at 1mM, pH 6 and at 22–23 °C.

Sample/contrast	Layer	$\tau\pm2/\text{\AA}$	$(\rho_{po}\pm0.1)\times10^{-6}/\text{\AA}^2$	$(\rho_p\pm0.1)\times10^{-6}/\text{\AA}^2$	$\phi_p\pm0.05$	$\Gamma\pm0.15/\text{mg m}^{-2}$	$\Gamma_{total}\pm0.15/\text{mg m}^{-2}$	$A\pm2/\text{\AA}^2$
h $C_{14}hK_2/D_2O$	h C_{14}	13	-0.05	0.5	0.91	1.03	2.23	36.1
	h K_2	13	3.33	4.2	0.71	1.20		
d $C_{14}hK_2/D_2O$	d C_{14}	13	6.91	6.85	0.82	1.04	2.07	40.9
	h K_2	11	3.33	4.2	0.72	1.03		
d $C_{14}hK_2/CMSi$	d C_{14}	13	6.91	6.0	0.81	1.04	2.07	40.9
	h K_2	11	1.85	1.9	0.73	1.03		
d $C_{14}hK_2/H_2O$	d C_{14}	13	6.91	5.3	0.79	1.00	2.04	41.5
	h K_2	11	0.95	0.55	0.74	1.04		

Table S6 C₁₄K₃ structural parameters obtained from 2-layer model fitting to neutron reflectivity profiles measured at the C8/water interface. The C8 layer was determined from pure D₂O with $\tau=11\pm3 \text{ \AA}$ and $\rho=1.4\times10^{-6}/\text{\AA}^2$. All the measurements were made at 3mM, pH 6 and at 22–23 °C.

Sample/contrast	Layer	$\tau\pm2/\text{\AA}$	$(\rho_{po}\pm0.1)\times10^{-6}/\text{\AA}^{-2}$	$(\rho_p\pm0.1)\times10^{-6}/\text{\AA}^{-2}$	$\phi_p\pm0.05$	$\Gamma\pm0.15/\text{mg m}^{-2}$	$\Gamma_{total}\pm0.15/\text{mg m}^{-2}$	$A\pm2/\text{\AA}^2$
hC ₁₄ hK ₃ /D ₂ O	hC ₁₄	10	-0.05	1.7	0.73	0.63	1.72	59.5
	hK ₃	12	3.33	4.2	0.71	1.08		
dC ₁₄ hK ₃ /D ₂ O	dC ₁₄	12	6.91	6.7	0.64	0.74	1.82	58.4
	hK ₃	12	3.33	4.2	0.71	1.08		
dC ₁₄ hK ₃ /CMSi	dC ₁₄	12	6.91	5.2	0.65	0.76	1.84	58.4
	hK ₃	12	1.83	1.9	0.71	1.08		
dC ₁₄ hK ₃ /H ₂ O	dC ₁₄	12	6.91	4.2	0.64	0.74	1.82	58.4
	hK ₃	12	0.94	0.5	0.71	1.08		

Table S7 C₁₄K₄ structural parameters obtained from 2-layer model fitting to neutron reflectivity profiles measured at the C8/water interface. The C8 layer was determined from pure D₂O with $\tau=11\pm3 \text{ \AA}$ and $\rho=1.4\times10^{-6}/\text{\AA}^2$. All the measurements were made at 4mM, pH 6 and at 22–23 °C.

Sample/contrast	Layer	$\tau\pm2/\text{\AA}$	$(\rho_{po}\pm0.1)\times10^{-6}/\text{\AA}^{-2}$	$(\rho_p\pm0.1)\times10^{-6}/\text{\AA}^{-2}$	$\phi_p\pm0.05$	$\Gamma\pm0.15/\text{mg m}^{-2}$	$\Gamma_{total}\pm0.15/\text{mg m}^{-2}$	$A\pm2/\text{\AA}^2$
hC ₁₄ hK ₄ /D ₂ O	hC ₁₄	9	-0.05	1.8	0.71	0.55	1.91	64.5
	hK ₄	14	3.30	4	0.77	1.36		
dC ₁₄ hK ₄ /D ₂ O	dC ₁₄	8	6.91	6.75	0.73	0.56	1.72	74.3
	hK ₄	12	3.30	4	0.77	1.16		
dC ₁₄ hK ₄ /CMSi	dC ₁₄	8	6.91	5.6	0.73	0.57	1.71	75.1
	hK ₄	12	1.82	1.88	0.76	1.14		
dC ₁₄ hK ₄ /H ₂ O	dC ₁₄	8	6.91	4.8	0.72	0.56	1.7	75.1
	hK ₄	12	0.93	0.57	0.76	1.14		

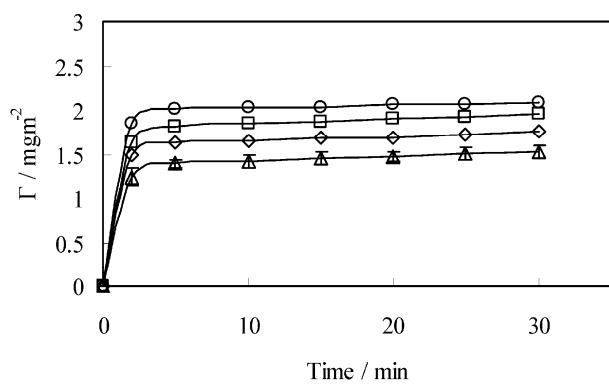


Fig. S1 Interfacial adsorption of lipopeptide surfactants plotted as surface adsorbed amount expressed in mg m^{-2} versus time at the hydrophobic solid /water interface at the concentration of above CMC , pH 6 and 22-23 °C: $C_{14}K_1$ (○, 1mM), $C_{14}K_2$ (□, 1mM), $C_{14}K_3$ (△, 3mM), and $C_{14}K_4$ (◊, 4mM). The continuous line is drawn to guide the eyes.

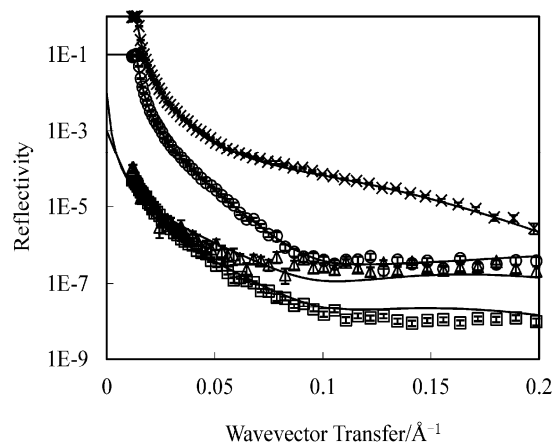


Fig. S2 2-layer layer model fitting to $C_{14}K_2$ monolayer adsorbed at the C_8 /water interface: $hC_{14}hK_2$ in D_2O (×) $dC_{14}hK_2$ in D_2O (○); $dC_{14}hK_2$ in D_2O-H_2O mixture ($\rho = 2.07 \times 10^{-6} \text{ \AA}^{-2}$) (△) and $dC_{14}hK_2$ in H_2O (□). All the measurements were made at 1mM, pH 6 and at 22-23°C. Symbols represent the measured data; continuous lines represent the best fits. .

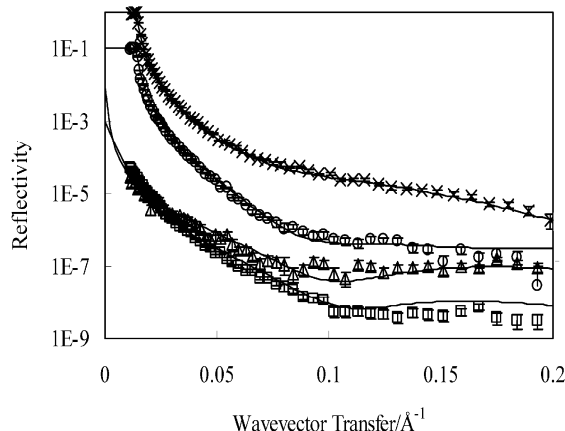


Fig. S3 2-layer layer model fitting to $C_{14}K_3$ monolayer at the C_8 /water interface: $hC_{14}hK_3$ in D_2O (\times) $dC_{14}hK_3$ in D_2O (\circ); $dC_{14}hK_3$ in D_2O-H_2O mixture ($\rho = 2.07 \times 10^{-6}$ Å²) (Δ) and $dC_{14}hK_3$ in H_2O (\square). All the measurements were made at 3mM, pH 6 and at 22-23°C. Symbols represent the measured data; continuous lines represent the best fits.

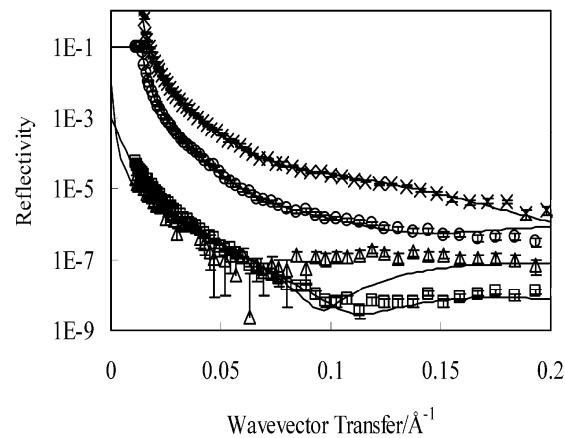


Fig. S4 2-layer layer model fitting to $C_{14}K_4$ monolayer adsorbed at the C_8 /water interface: $hC_{14}hK_4$ in D_2O (\times) $dC_{14}hK_4$ in D_2O (\circ); $dC_{14}hK_4$ in D_2O-H_2O mixture ($\rho = 2.07 \times 10^{-6}$ Å²) (Δ) and $dC_{14}hK_4$ in H_2O (\square). All the measurements were made at 4mM, pH 6 and at 22-23°C. Symbols represent the measured data; continuous lines represent the best fits.